TISSUE ENGINEERING: Part A
Volume 19, Numbers 19 and 20, 2013

DOI: 10.1089/ten.tea.2012.0565

In Vitro Development and Characterization of a Tissue-Engineered Conduit Resembling Esophageal Wall Using Human and Pig Skeletal Myoblast, Oral Epithelial Cells, and Biologic Scaffolds

Tigran Poghosyan, MD, PhDc,[1–3] Sebastien Gaujoux, MD, PhD,[1,2] Valerie Vanneaux, Pharm D, PhD,[1,3] Patrick Bruneval, MD, PhD,[4] Thomas Domet, MSc,[1,3] Severine Lecourt, PhD,[1,3] Mohamed Jarraya, MD,[5] Rony Sfeir, MD,[6] Jerome Larghero, Pharm D, PhD,[1,3] and Pierre Cattan, MD, PhD[1–3]

Introduction: Tissue engineering represents a promising approach for esophageal replacement, considering the complexity and drawbacks of conventional techniques.
Aim: To create the components necessary to reconstruct *in vitro* or *in vivo* an esophageal wall, we analyzed the feasibility and the optimal conditions of human and pig skeletal myoblast (HSM and PSM) and porcine oral epithelial cell (OEC) culture on biologic scaffolds.
Materials and Methods: PSM and HSM were isolated from striated muscle and porcine OECs were extracted from oral mucosa biopsies. Myoblasts were seeded on an acellular scaffold issue from porcine small intestinal submucosa (SIS) and OEC on decellularized human amniotic membrane (HAM). Seeding conditions (cell concentrations [0.5×10^6 versus 10^6 cells/cm^2] and culture periods [7, 14 and 21 days]), were analyzed using the methyl thiazoltetrazolium assay, quantitative PCR, flow cytometry, and immunohistochemistry.
Results: Phenotypic stability was observed after cellular expansion for PSM and HSM (85% and 97% CD56-positive cells, respectively), and OECs (90% AE1/AE3- positive cells). After PSM and HSM seeding, quantities of viable cells were similar whatever the initial cell concentration used and remained stable at all time points. During cell culture on SIS, a decrease of CD56-positive cells was observed (76% and 76% by D7, 56% and 70% by D14, 28% and 60% by D21, for PSM and HSM, respectively). Multilayered surface of α-actin smooth muscle and Desmine-positive cells organized in bundles was seen as soon as D7, with no evidence of cell within the SIS. Myoblasts fusion was observed at D21. Pax3 and Pax7 expression was downregulated and MyoD expression upregulated, at D14.OEC proliferation was observed on HAM with both cell concentrations from D7 to D21. The cell metabolism activity was more important on matrix seeded by 10^6 cells/cm^2. With 0.5×10^6 OEC/cm^2, a single layer of pancytokeratin-positive cells was seen at D7, which became pluristratified by D14, while when 10^6 OEC/cm^2 were used, a pluristratified epithelial structure was seen as soon as D7. Proliferative cells (Proliferating Cell Nuclear Antigen staining) were mainly located at the basal layer.
Conclusion: In this model, the optimal conditions of cell seeding in terms of cell concentration and culture duration were 0.5×10^6 myoblasts/cm^2 and 10^6 OEC/cm^2, and 7 days.

Introduction

Esophageal replacement for benign or malignant diseases such as esophageal carcinoma, caustic injuries, or long-gap esophageal atresia, usually involves gastric or colonic interposition.[1–5] These reconstructions have a significant early and late morbidity and functional results are often disappointing.[6]

An alternative therapeutic approach such as interposition of synthetic materials has invariably lead to anastomotic

This work was presented, in part, as an oral communication at the following meetings: Strategies in Tissue Engineering (STE, 3rd International Conference), Abstract O-144, May 23–25, 2012, Wurzburg, Germany. European Society for Surgical Research (ESSR 2012, 47th Annual congress), Abstract OP-11, June 6–9, 2012, Lille, France.
[1]Cell Therapy Unit and Clinical Investigation Center in Biotherapies (CIC-BT501), Saint-Louis Hospital, AP-HP and University Paris Diderot, Sorbonne Paris Cité, Paris, France.
[2]Department of Digestive, General and Endocrine Surgery, Saint-Louis Hospital, AP-HP, Paris, France.
[3]INSERM UMR 940, Institut Universitaire d'Hématologie, Saint-Louis Hospital, Paris, France.
[4]Department of Pathology, Georges Pompidou European Hospital, AP-HP, Paris, France.
[5]Human Tissue Bank, Saint-Louis Hospital, AP-HP, Paris, France.
[6]Department of Pediatric Surgery, Jeanne de Flandre Hospital and University Lille 2, Lille, France.

dehiscence and their extrusion, because of their poor biocompatibility.[7,8] Despite few attempts, esophageal allograft is not a realistic option due to the complexity of the vascular anatomy of the esophagus and the need of long-term immunosuppression.[9] Previously, we assessed the capacity of an allogeneic aortic allograft to bridge a short cervical esophageal gap in a porcine model. The high fibrotic reaction, the absence of contractility, and the propulsive capacity of the graft area limit the application of this technique to short segmental defect replacement.[10] Other tissue such as pleura, pericardium, muscle, and skin have been used as autografts with similar disappointing results.[11]

The concept of tissue engineering is based on the *in vitro* or/and *in vivo* association of cells and acellular matrix for the reconstruction of an organ or tissue.[12] This concept, which has already been applied to humans for bladder and tracheobronchial replacement[13,14] and venous leg ulcers treatment,[15] brings several theoretical advantages for esophageal replacement such as preservation of native intra-abdominal conduits, replacement tailored to the exact length of the esophageal defect or disease, and the absence of immunosuppression because of the acellular nature of the matrix and the autologus nature of the cells. Over the last decade, several experimental models have been used in search of the ideal approach for esophageal regeneration by tissue engineering. The hybrid approach, which is based on the *in vitro* combination of different cell types and matrices, seems the most promising.[16,17]

Schematically, the histology of the esophageal wall is presented by two major components: the squamous epithelium and the muscular layer. The squamous epithelium, whose basal layer is mainly composed by cell progenitors participating in the renewal of the more superficial layers, is a protective barrier against salivary and peptic aggression. The role of the muscular layer is to propel the food bolus. The muscular layer of the upper third of the esophagus is composed of striated muscles fibers. The myoblasts, which are located between the plasmatic membrane and the basal lamina of striated muscle fibers possess a strong myogenic capacity and are currently considered as one of the main sources of striated muscles cells.

The choice of the scaffolds is also important. Naturally derived accellular scaffolds contain intact structural proteins such as collagen, fibronectin, laminin, glycosaminoglycans, and different growth factors in their native three-dimensional form, improving cell adhesion, growth, proliferation, and differentiation.[18]Acellular scaffolds issue from the porcine small intestinal submucosa (SIS) and decellularized human amniotic membrane (HAM) seem the most promising to reach our goal.[18–21]

In the aim to prepare *in vitro* an esophageal substitute according to an hybrid approach, we analyzed the feasibility and the optimal conditions of cell seeding as well as the phenotypic behavior of the porcine and human skeletal myoblasts (PSM and HSM) on SIS and of porcine oral epithelial cells (OEC) on a decellularized HAM.

Materials and Methods

Animals care and anesthesia

Minipigs aged 2 years and weighing 25 to 30 kg were used (Le Noyer, Bretoncelles 61110, France). All animals received care in accordance with the *Guide for the Care and Use of Laboratory Animals* from the Institute of Laboratory Animal Resources, National Research Councils, and published by the National Academy Press, revised 1996, and with French regulations and institutional ethics committee guidelines for animal research.

Anesthesia

Animals underwent a 12-h diet and an intramuscular injection of ketamine (10 mg/kg), 30 min before induction. After induction with intravenous propofol (1%; 8 mg/kg) and endotracheal intubation, ventilation was performed with a Siemens 900 C ventilator (Siemens; tidal volume 10 mL/kg, 24 breaths/min). Anesthesia was maintained with inhaled 60% oxygen and 1% to 2% isoflurane until the end of the procedure. Animals were perfused with a crystalloid solution (10 mg/kg/h).

Tissue biopsies

A right quadricipital sampling (average weight 3.5 g) and buccal mucosa sampling (average weight 2.5 g) were performed for pig myoblast and OEC isolation, respectively. Samples were preserved in a solution of 9% NaCl at 4°C, until processing. Human skeletal muscle biopsies were obtained via the Tissue Bank for Research of the French Association against myopathy in the context of approved clinical trials in agreement with the French bioethical low (Law n°94-654 of the 29 July 1994, modified the 22 January 2002). Biopsies were 0.3–4 g. *res nullius* specimen from orthopedic surgery. The donors were adults and had no clinical signs of muscular diseases.

Myoblast isolation and characterization

Muscle biopsies were enzymatically dissociated and cells were cultured in a proliferation medium promoting the expansion of CD56 myogenic cells as previously described.[22] Myoblasts were phenotyped by staining with the anti-CD56 (1/50, Becton Dickinson®, NCAM clone 6.2, mouse Ig2b PE) and the anti-Desmine primary antibodies (1/50, Becton Dickinson) revealed by the secondary goat anti-mouse antibody (1/100, FITC). Cells without myogenic abilities were sought by anti-CD15 antibodies (1/50 Becton Dickinson, clone MMA, mouse IgM, FITC). Data were acquired and analyzed on a five-parameter flow cytometer (FACScalibur; Becton Dikkinson) with CellQuestPro software (Becton Dickinson). At least 10^4 events were analyzed for each sample.

OECs isolation and characterization

OEC isolation was performed by using the method described by Beckstead*et al.*,[23] with modifications. The buccal mucosa biopsy was weighed and immersed for a few seconds in an iodide solution diluted to half with 1Xphosphate-buffered saline (PBS) (Invitrogen), and then rinsed two times in 1XPBS. The epithelium was separated from any outstanding underlying muscle or connective tissue and minced using sterile microsurgical instruments, and then incubated for 2 h in Dispase I, (50 mg/mL; Roche). The enzymatic digestion was terminated by incubating the minced tissue during 20 min in a trypsin-EDTA 1X solution (Invitrogen) at

37°C, 5% CO_2. The resulting suspension was filtered and centrifuged. The cell pellet was resuspended and cultured at 10^4 cells/cm^2 in a culture medium (OEC medium) containing the Dulbecco's modified Eagle's medium high glucose (Sigma Aldrich) and fetal bovine serum (FBS) (10%, ThermoFisher Hyclone) supplemented with 10 ng/mL human recombinant epithelial growth factor (Carier Free, DR Systems), 5 μg/mL Apo-Transferrin (Apo-Transferrin human cell culture test, Sigma Aldrich), 0.4 μg/mL hydrocortisone hemisuccinate, 10 μg/mL insulin, 50 μg/mL gentamycin, and 1Xpenicillin-strepromycin-glutamine (antibiotics/antimycotics, Sigma Aldrich) at 37°C, 5% CO_2. The culture medium was changed every 48 h. Cells were passed at 60%–80% of confluence. After each passage, cells were grown at 5×10^3cells/cm^2. At the first passage and before cell seeding on a matrix, the cell phenotype was analyzed by immunohistochemistry (cytospin) using an anti-pancytokeratin antibody: AE1/AE3 (AE1/AE3 pancytokeratin 1/50 Dako).

Acellular scaffolds

The Surgisis® Soft Tissue Graft (Cook Medical) four-layers, 7×10 cm extracted from porcine SIS was used for PSM and HSM seeding (Fig. 1A).

HAM used for OEC seeding was provided for nontherapeutic use by the Tissue Bank of Assistance Publique–Hopitaux de Paris (Hôpital Saint-Louis) (Fig. 1B). Before use, HAM was decellularized from its native epithelium by enzymatic digestion (Fig. 1C).[24] Briefly, the HAM was thawed, washed three times in 1XPBS supplemented with levofloxacin, and cut into samples of 2 cm^2. Each sample was fixed on an insert (Scaffdex 24), and incubated for 8 min in a thermolysin solution 125 μg/mL (Thermolysin from *Bacillus Thermoproteolyticusrokko* Sigma Aldrich).

Cell seeding on acellular matrix

SIS samples were placed in Petri dishes and samples of decellularized HAM were fixed on inserts (Scaffdex 24). Then, scaffolds were covered for 24 h before cell seeding by specific culture media. The medium was removed before cell seeding. Then, 50 μL of cell suspension was laid on each matrix sample, and incubated at 37°C, 5% CO_2 for 1 h. The culture medium was then added to cover the scaffold and was changed every 2 days.

Cell viability and proliferation analysis

Cell viability and proliferation after cell seeding were analyzed using the methyl thiazoltetrazolium (MTT) assay. Scaffolds with or without cell seeding (control group) were incubated at 37°C, 5% CO_2 for 3 h into 300 μL of the MTT solution (1%). The scaffolds were then incubated for 10 min in 300 μL of isopropanol (96%). A sample of 100 μL was transferred to a 96-well microplate and the absorbance was read at 570 nm. The obtained optical density values were correlated with the number of living cells through the production of a calibration curve for each experiment.

Phenotypic stability analysis

PSM and HSM were extracted at different time points from the SIS by trypsinization and phenotyped by FACS analysis after staining with anti-CD56, anti-Desmine, and anti-CD15.

Histological and immunocytochemistry analysis

Seeded scaffolds, fixed in 4% paraformaldehyde, were included in paraffin. Histological sections of 4 μm followed by hematoxylin erythrosine saffron (HES) staining were performed. For immunohistochemistry analysis, antigen retrieval was performed by heating the tissue sections in a 0.1 M citrate buffer, pH 6.0. Immunostaining was performed in a Ventana processor (Ventana, Illkirsh, France).

For SIS seeded with myoblasts, anti-Desmine (Desmine D33;Dako) and α-Actin smooth muscle antibody (1/100, α-ASM, Clone1A4;Dako) were used.

For HAM seeding with OEC, staining was performed using anti-pancytokeratin AE1/AE3 and a proliferating cell nuclear antigen (PCNA, Clone PC10; Dako) staining.

RNA extraction and quantitative PCR

HSM was collected before seeding (day 0, D0) and from SIS at D7 and D14 of culture. Total RNA was extracted with RNeasy mini kit (Qiagen). Reverse transcription Quantitative PCR was performed with TaqMan® Gene Expression Assays on an ABI7500 (Applied Biosystems). *Pax3, Pax7, MyoG, MyoD*, and *GAPDH* (endogenous control) expression were assessed (predesigned assays, references, respectively: Hs00240950_m1; Hs00242962_m1; Hs01072232_m1; Hs00159528_m1; and Hs99999905_m1). The $2^{-\Delta\Delta Ct}$ method was used and results expressed as gene expression fold increase relative to Day 0. The $2^{-\Delta\Delta Ct}$ value between 0.5 and 2 was considerate as stable expression.

Study design and statistical analysis

To analyze the best conditions of cell seeding and cell culture on a matrix, two myoblasts and OEC concentrations ($0.5\times10^6$and 10^6 cells/cm^2) and three delay of culture period on the matrix (7, 14, and 21 days) were tested. Cell viability and proliferation, phenotype stability, and architecture of the construct were analyzed under these different

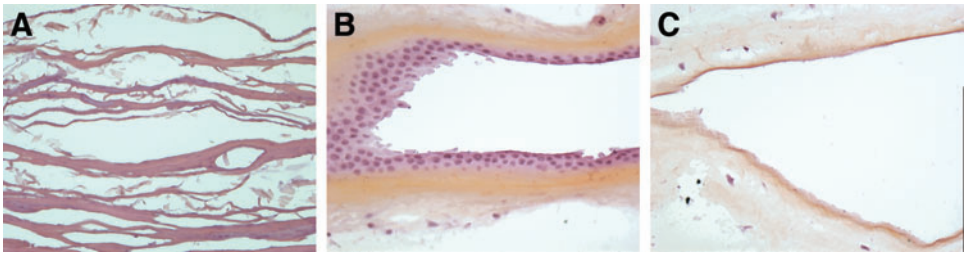

FIG. 1. **(A)** Small intestinal submucosa (SIS) (Hematoxylin Erythrosine Saffron [HES]×20); **(B)** Human amniotic membrane (HAM) with native epithelium (HES×20); **(C)** Decellularized HAM (HES×20). Color images available online at www.liebertpub.com/tea

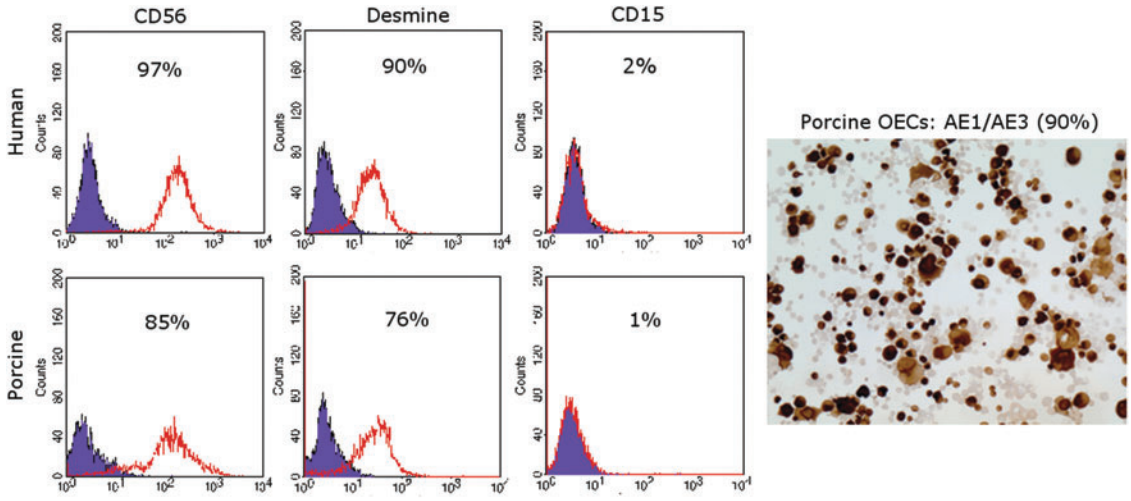

FIG. 2. Flow cytometry analysis of CD56, Desmine, and CD15 expression on human and porcine skeletal myoblasts (HSM and PSM) after cell expansion. Immunohistochemical staining (AE1/AE3) of porcine oral epithelial cell (OEC) after cell expansion. Color images available online at www.liebertpub.com/tea

conditions. In all cases, each experimental protocol was performed at least three times, and in a triplicate condition for each experiment. Data are expressed as mean ± standard deviation. The unpaired, one-tail *t*-Student test was used when necessary. *p*-Values ≤ 0.05 were considered statistically significant.

Results

Myoblasts and OEC isolation and expansion

Phenotype analysis of PSM performed at passage 4, showed a stable phenotype with an average of 85% (±5) CD56 and 76% (±12) Desmine-positive cells. The rate of CD15-positive cells, was <1% (Fig. 2). Concerning HSM, the mean rate of CD56-, Desmine-, and CD15-positive cells were 97% (±1), 90% (±3), and 2% (±2), respectively (Fig. 2). At passage 3 of OECs, the mean percentage of AE1/AE3-positive cells was 90% (±10) (Fig. 2).

Myoblasts seeding on SIS

Cell viability and proliferation. MTT assay showed a significant cell loss following seeding at early time points (between D0 and D7) for porcine and human cell types (Fig. 3A,B). For PSM (Fig. 3A), the metabolic activity was similar for both cell concentrations, at all time points. However, a gradual significant and parallel increase of metabolic activity was observed from D7 until D21, for both cell concentrations. Regarding HSM, cell metabolism was significantly higher at D7 when 10^6 cells/cm^2 cell were seeded, compared to 0.5×10^6 cells/cm^2, this difference disappeared thereafter. The metabolic activity remained stable and similar whatever the initial cell concentration at the following time points (Fig. 3B).

Flow cytometry analysis. Phenotype analysis of the PSM extracted from the SIS at various time points showed a progressive significant decrease of the CD56- and Desmine-positive cell rates (Fig. 4). The rate of CD15-positive cells remained minimal at all time points (1%–2%).

With HSM, a similar trend in the loss of CD56- and Desmine-positive cells during culture on SIS was observed, but was less pronounced compared to PSM. Parallel phenotype analysis of the same HSM population cultured in a Petri dish and passed at 60%–80% of confluence, showed a more stable CD 56 and Desmine expression during this period, while a loss of myoblast phenotype was observed when cells were cultured at 100% of confluence (Fig. 5A,B).

To distinguish between the potential role played by the scaffold and cell over density in the loss of myoblast phenotype during culture on the matrix, HSM was extracted from the SIS after a 14-day culture period, secondarily put in the Petri dish for 14 days, and passed at 60%–80% of confluence. From cell extraction from the SIS to a 14-day culture in the Petri dish, the average rates of CD56- and Desmine-positive cells increased by more than 20% and were similar to the CD56 and Desmine rates of primarily cultured myoblasts at 60%–80% of confluence by day 28 (Fig. 5A,B).

Quantitative PCR finding. Expressions of *Pax3*, *Pax7*, and *MyoG* were stable at D7 when compared to D0, while a downexpression of MyoD was observed (Fig. 6). At D14, *MyoG* expression remained stable, while an important downregulated expression was observed for *Pax3* and *Pax7*. In parallel, *MyoD* expression was upregulated.

Histological and immunohistochemical findings. For both PSM and HSM, HES staining of the construct showed a multilayered surface (5–6 cell layers) composed of mononuclear fusiform cells organized in bundles, covering the entire surface of the scaffold by D7 (Fig. 7). There was no evidence of cells within the SIS (Fig. 7A–D and I–L). Myoblast fusion and multinucleate myotube formation were observed with human cells after 21 days of culture on SIS (Fig. 7G, H). Immunohistochemical analysis showed a low anti α-ASM staining (Fig. 7 M–P—only porcine cells staining are shown). Desmine-positive staining was observed in seeded HSM (Fig. 7E–H), while it was negative in PSM because of noncrossing antibodies (data not shown).

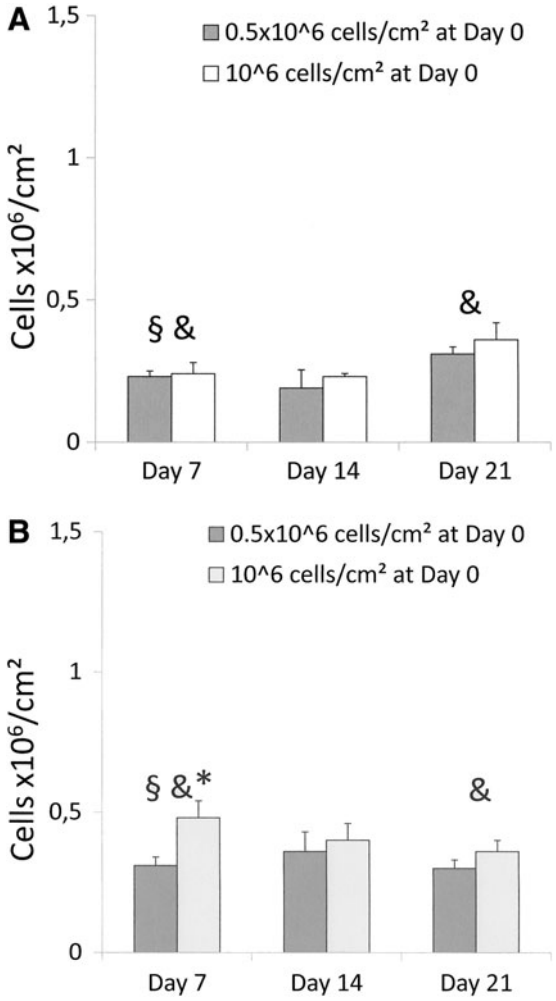

FIG. 3. Methyl thiazoltetrazolium (MTT) assay. Cell viability and proliferation analysis after seeding of two cell concentrations (0.5×10^6 cells/cm^2 and 10^6 cells/cm^2) and performed at three time points (D7, D14, and D21) **(A)** PSM: §, D0 versus D7 for both concentrations ($p<0.001$); &, D7 versus D21 ($p=0.01$ for 0.5×10^6cells/cm^2 and $p=0.04$ for 10^6cells/cm^2). **(B)** HSM: §, D0 versus D7 ($p=0.028$ for 0.5×10^6cells/cm^2 and $p<0.001$ for 10^6cells/cm^2); &, D7 versus D21 for 10^6 cells/cm^2 ($p=0.04$). *, between the two cell concentrations at D7 ($p=0.04$).

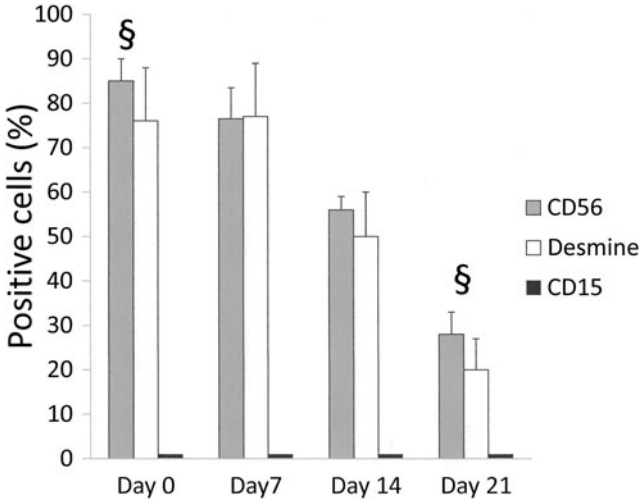

FIG. 4. Flow cytometry analysis of PSM phenotype: §, D0 versus D21 for CD56 ($p<0.001$) and Desmine ($p=0.002$) rates.

OEC seeding on HAM

Cell viability and proliferation. A significant loss of seeded cells was observed at the earliest time point for both cell concentrations. The numbers of viable cells were significantly higher on scaffolds seeded at 10^6/cm^2 at all time points. With both concentrations, a significant increase in the number of viable cells was observed between D7 and D21 (Fig. 8).

Histological and immunohistochemical findings. After HES staining, architectural analysis of the samples seeded with 0.5×10^6 cell/cm^2 showed a cell monolayer covering the entire surface of the membrane at D7 (Fig. 9A). This aspect became pluristratified from D14 (Fig.9B). At that time point, an epithelial morphology consisting in cube-shaped cells surrounded by flat cells was observed. Architectural analysis of the samples seeded at 10^6 cell/cm^2 showed a multilayer structure as soon as D7 (5–6 layer) (Fig. 9C) with an increased number of layers at D14 (Fig. 9D) and D21. Pan-cytokeratin (AE1/AE3) staining was positive at all time points and proliferating (PCNA-positive) cells were mainly, but not exclusively, localized at the basal layer (Fig. 9E–H).

Discussion

There are several arguments suggesting that the addition of cells to a natural acellular scaffold is essential to achieve tissue remodeling in the setting of esophageal tissue engineering. In fact, circumferential replacement of the esophagus with an acellular scaffold, systematically lead to the formation of a stenosis.[25–27] After patch esophagoplasty[28] and circumferential esophageal replacement,[29] the addition of muscle cells to the matrix reduces the local inflammatory response and enhances the tissue remodeling process. While most authors use smooth muscle cells,[16,28,30] we chose skeletal myoblast, because of their capacity to differentiate into striated muscle and to promote regeneration of damaged muscle fibers.[31,32] In case of muscular dystrophy, it was found that the injection of healthy myoblasts could not only amend the genetic profile of dystrophic muscle by fusing with the deficient fibers, but also increase their contractile capacity.[33,34] Skeletal myoblasts are precursor cells of adult myofibers and feature several advantages, including autologous origin, high *in vitro* scalability, and a lack of tumorigenicity due to myogenic lineage restriction. We have already shown that autologous skeletal myoblast transplantation is a feasible and straightforward procedure, and demonstrated that myoblast culture could be clinically upgraded rendering them compatible with human use.[35,36]

On the other hand, it has been shown that autologous epithelial cell sheets protect extensive esophageal mucosectomy from stricture development by accelerating the healing process and reducing submucosal inflammation.[37]

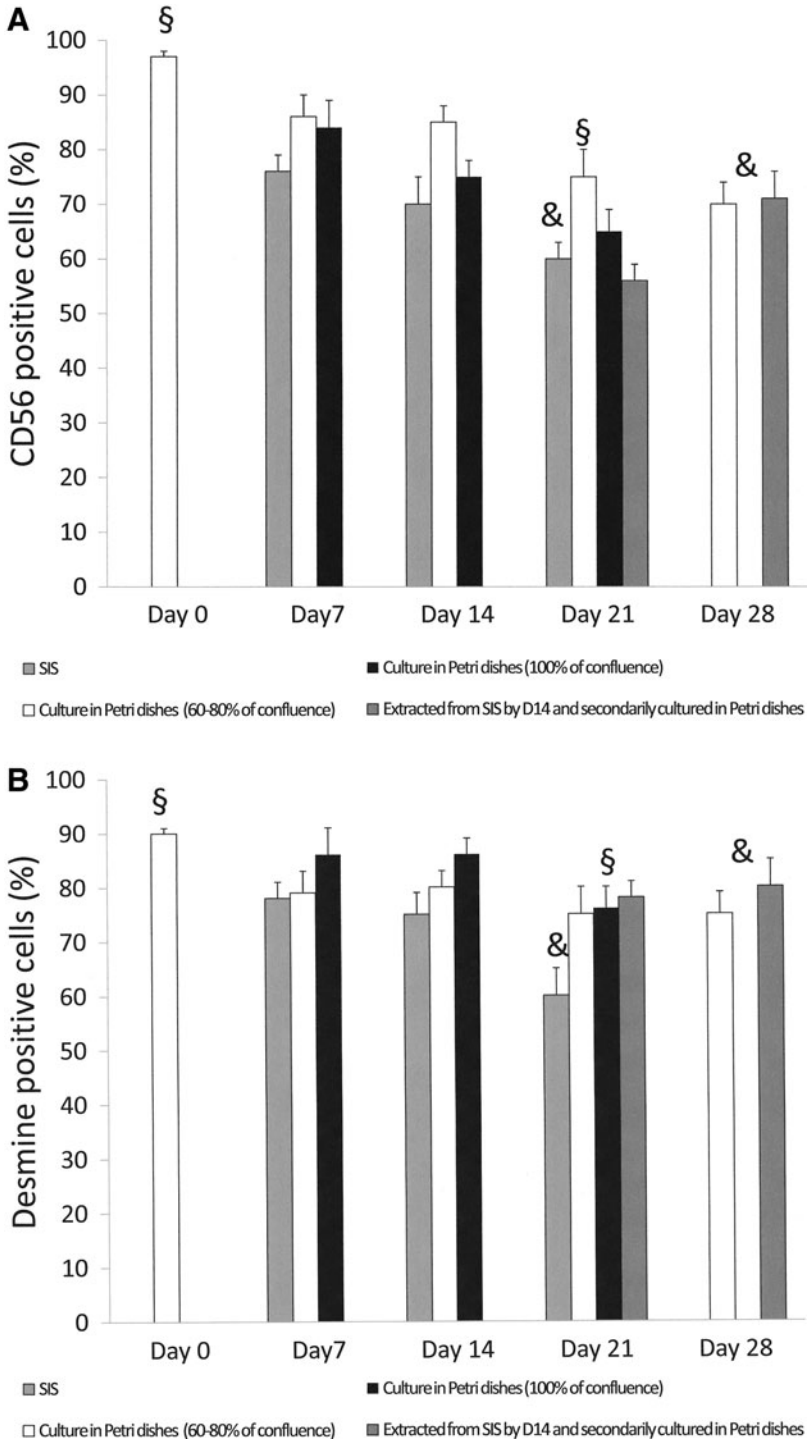

FIG. 5. Flow cytometry analysis of HSM phenotype. **(A)** Mean rate of CD56-positive cells according to different culture conditions: §, D0 versus D21 for all conditions ($p < 0.001$); & D21 (cells cultured on SIS) versus Day 28 (cells cultured at 60%–80% of confluence [$p = 0.025$] and cells cultured in Petri dishes for 14 days at 60%–80% of confluence after extraction from SIS at D14 [$p = 0.03$]). **(B)** Mean rate of Desmine-positive cells according different culture conditions: §, D0 versus D21 for all conditions ($p < 0.01$); &, D21 (cells seeded on SIS) versus Day 28 (cells extracted from SIS by D14 and secondarily cultured in Petri dishes during 14 days at 60%–80% of confluence ($p = 0.034$).

Epithelial cells accelerate muscle regeneration in a patch esophagoplasty model.[38] Finally, these cells protect against stenosis after circumferential esophageal replacement by a substitute composed of polyglycolic acid and smooth muscle cells.[17] In view of these observations, it seems that communications between different cell types and the matrix are beneficial to tissue remodeling; therefore, the hybrid approach, consisting in assembling acellular scaffolds seeded with epithelial and muscle cells, seems currently the most promising approach.[12,17,39,40]

Results of the present study allow us to draw some conclusions regarding the optimal conditions of matrix cell seeding in such a model. A high rate of early myoblast loss was observed when a concentration of 10^6 cells/cm^2 was used. In a study analyzing the seeding of mouse myoblasts on SIS at a concentration of 0.5×10^6 cells/cm^2, Wolf *et al.*[41] showed that cell metabolism decreased at Day 1 and subsequently doubled at Day 5. In our hands, such a kinetic at early time points was not confirmed, since we observed a similar MTT activity at D3 and D7 after seeding 0.5×10^6

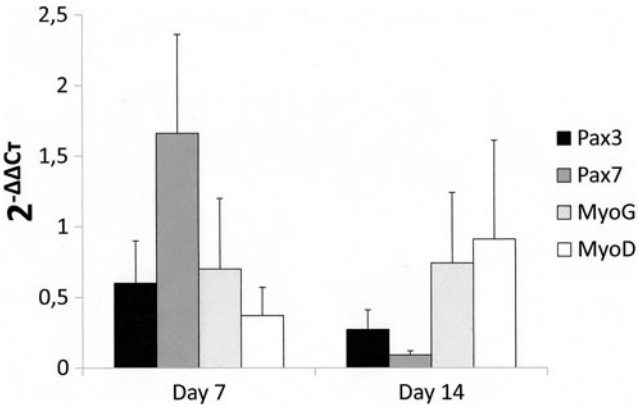

FIG. 6. Expression of *Pax3, Pax7, MyoG*, and *MyoD* at D7 and D14. The $2^{-\Delta\Delta Ct}$values of *Pax3, Pax7, MyoG*, and *MyoD* at D0 are considerate as 1.

cells/cm^2 (data not shown). In comparison to 10^6 cells/cm^2, we did not observe such a loss, when 0.5×10^6 cells/cm^2 were used. This suggests that high cell concentration compromises cell adhesion, and may also promote cell death.

Another conclusion issue from our experiments is that the myoblast cell population do not expand on SIS between D7 and D21. This absence of sizeable cell expansion was confirmed by histology, showing pluristratified cellular structures covering the surface of the scaffold by D7, whose architecture remained unchanged with time, whatever the cell concentration used. To analyze that phenomenon, cell expansion after the seeding of 5×10^4 cells/cm^2 was analyzed at D3, D7, and D14 (data not shown). The cell number was stable at D3 (6×10^4 cells/cm^2), and a progressive increased number of cells was observed at D7 (13×10^4 cells/cm^2) and D14 (22×10^4 cells/cm^2), thus suggesting a role of steric hindrance in the limitation of cell expansion when higher cell concentrations were used.

Phenotypic analysis of cells sequentially extracted from the SIS showed a gradual decrease in CD56 and Desmine expression, less pronounced for human than for porcine cells. CD15 labeling, a marker of cells without myogenic abilities, still remained poorly detectable at all time points. This loss of the myoblast phenotype could be explained either by a decrease in extracellular cell surface marker expression, due to high cell density, or by myoblast differentiation. To explore the former hypothesis, the level of CD56-positive human

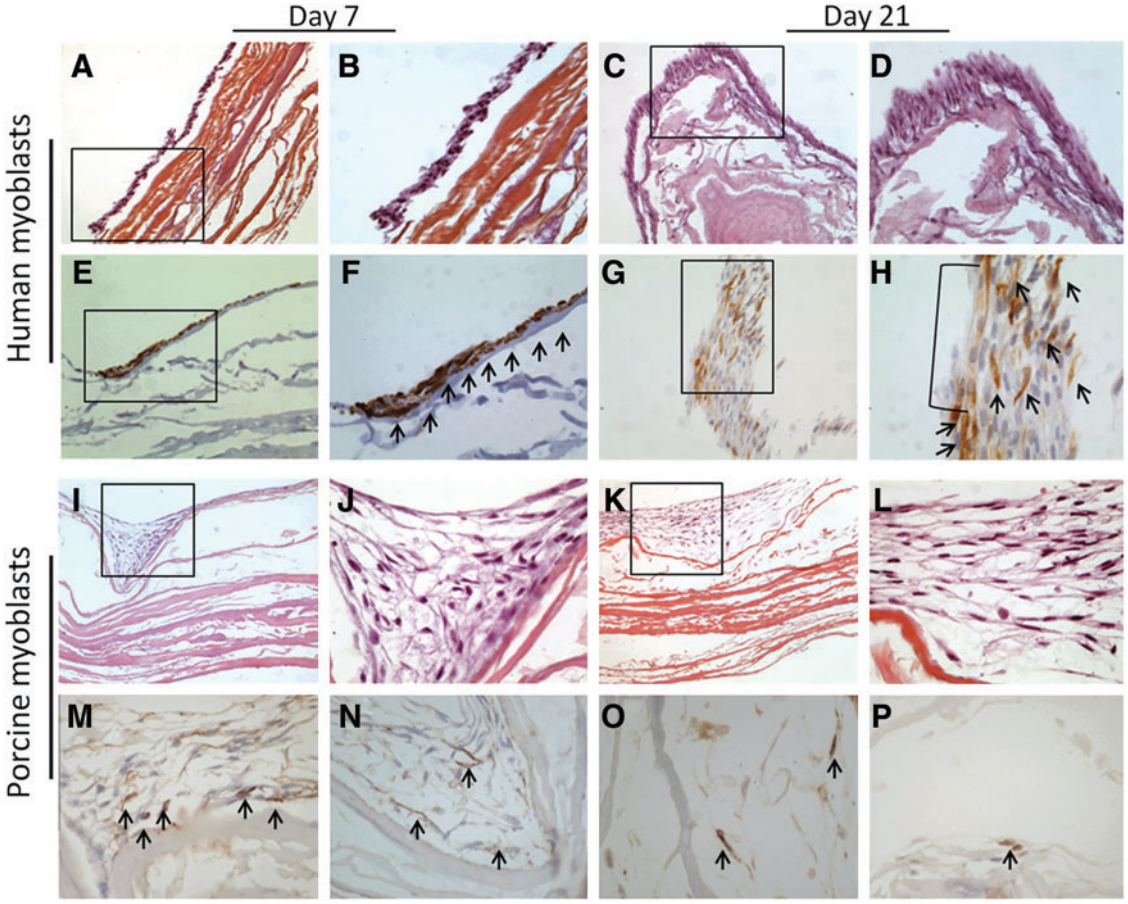

FIG. 7. Pathology analysis. **(A, B)** HSMs on SIS by D7 (HES×20 and×40); **(C, D)** HSMs on SIS by D21 (HES×20 and×40); **(E, F)** HSMs on SIS by D7 (Desmine staining×20 and×40); **(G, H)** HSMs on SIS by D21. Multinucleate myotube. (Desmine staining×20 and×40). **(I, J)** PSMs on SIS by D7 (HES×10 and×40); **(K, L)** PSMs on SIS by D21 (HES×10 and×40); **(M, N)** PSMs on SIS by D7 (α-smooth muscle actin[SMA] staining×20); **(O, P)** PSMs on SIS by D21 (α-SMA staining×20). Due to the absence of difference between two concentrations, only scaffolds seeded by 0.5×10^6 cells/cm^2 are shown. The arrows in **(F)** indicate desmin positive cells, the arrows in **(H)** indicate desmin positive cells and multinucleate myotube, and the arrows in **(M–P)** indicate SMA positive cells. Color images available online at www.liebertpub.com/tea

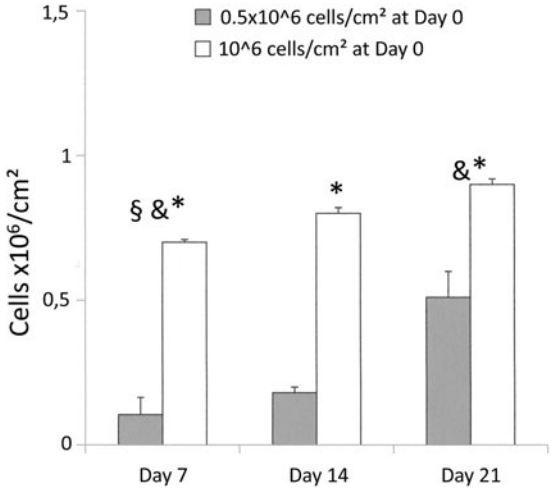

FIG. 8. MTT assay. OEC viability and proliferation analysis after seeding of two cell concentrations (0.5×10^6 cells/cm^2 and 10^6 cells/cm^2) and performed at three time points (D7, D14, and D21): §, D0 versus D7 for both cell concentrations ($p<0.001$); &, D7 versus D21 for both cell concentrations ($p=0.002$ for 0.5×10^6 cells/cm^2 and $p<0.001$ for 10^6 cells/cm^2). *, between two cell concentrations within same time points ($p<0.001$).

cells, cultured in three different conditions (on SIS, in Petri Dishes at 60%–80%, and at 100% confluence), were analyzed in parallel. While CD56 expression remained stable at 60%–80% confluence, a similar decrease in CD 56 expression was observed after culture on SIS and at 100% of confluence, suggesting that cell over-density could in part explain the loss of CD56 expression. This was confirmed by the fact that cells extracted from the SIS at D14 and subcultured in Petri dishes recovered a high CD56 expression, after 14 days in culture. The second hypothesis, myoblast differentiation, is sustained by the analysis of myogenic regulatory factor expression. Myoblasts are characterized by coexpression of *Pax3* and *Pax7*, transcription factors involved in the specification and maintenance of skeletal muscle progenitors.[42–44] In our hands, a strong downregulation of *Pax3* and *Pax7* was observed between D7 and D14, while *MyoG* expression remains stable and *MyoD* was upregulated. These data are consistent with previous published studies reporting that *Pax7* is rapidly downregulated in cells that commit to terminal differentiation.[45] In addition, *Pax7* and *MyoD* closely interact during myogenesis, the *Pax7:MyoD* ratio playing a critical role in cell fate determination and the *Pax7*-mediated repressed muscle differentiation being abolished when *MyoG* expression is induced.[45,46] These observations were concomitant with the appearance of multinucleate myotube formation after D14.

As shown by Wolf *et al.*,[41] this process can be accelerated by the use of a culture medium deprived of FBS and supplemented by 2% horse serum. We purposely did not use such a medium because differentiation of myoblasts into muscle cells becomes irreversible, while our main goal was to maintain their progenitor capacity before *in vivo* implantation.

Esophageal epithelial tissue engineering for esophageal replacement also represents an important issue. Two comparative works,[23,47] which used epithelial cells and scaffolds of different origins, state that the combination of native esophageal squamous cells with a natural scaffold brings the best results in terms of proliferation of the basal layer, epithelial stratification, and cell adhesion.

HAM is currently used in humans, especially in the treatment of ophthalmologic diseases, as a support and vector of epithelial cell cultures. HAM basal lamina contains collagen IV, V, and laminin, which promote epithelial cell adhesion, migration, and differentiation, prevent cell apoptosis and inhibit fibroblasts and myofibroblast adhesion and proliferation.[48]

To circumvent the risk of esophageal perforation or stricture due to tissue procurement, we choose to use OECs. This

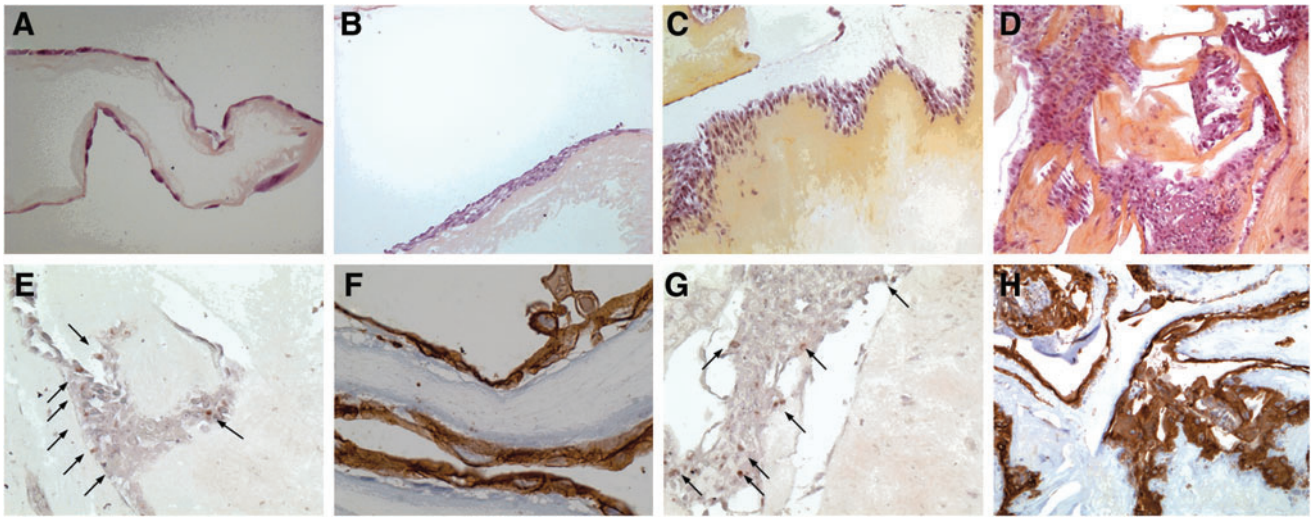

FIG. 9. Pathology analysis of porcine OEC on HAM **(A)** 0.5×10^6 cells/cm^2, D7 (HES×20); **(B)** 0.5×10^6 cells/cm^2, D14 (HES×10); **(C)** 10^6 cells/cm^2, D7 (HES×10); **(D)** 10^6 cells/cm^2, D14 (HES×10); **(E)** 0.5×10^6 cells/cm^2, D14 (Proliferating Cell Nuclear Antigen [PCNA]×20); **(F)** 0.5×10^6 cells/cm^2, D14 (pancytokeratin AE1/AE3×40); **(G)** 10^6 cells/cm^2, D14 (PCNA×20); **(H)** 10^6 cells/cm^2, D14 (pancytokeratin AE1/AE3×5). The arrows in **(E,G)** indicate PCNA positive cells. Color images available online at www.liebertpub.com/tea

protocol has already been used in circumferential replacement of the esophagus in a canine model with convincing histological and clinical results.[17] We obtained multilayered epithelial structures by D7 with 10^6 cells/cm^2, and by D14 with 0.5×10^6 cells/cm^2. The epithelial nature of these cells was confirmed by a AE1/AE3 strong positive staining at all time points. The utility of using feeder cells to enhance epithelial cell culture is still a matter of debate. Some authors cultivate squamous epithelial cells in the presence of the feeder cells (lethally irradiated mouse fibroblasts),[17,47] while others performed their culture without.[16,23] Although we did not use these cells, we obtained a pluristratified epithelium with a basal layer of proliferative cells.

This work represents the *in vitro* part of an experimental project of cervical esophageal replacement by tissue engineering in large animals. The pig model was chosen because of its accessibility and anatomical similarity with human. At the same time, and in prevision of future clinical studies, we analyzed whether human myoblasts behave as their porcine counterparts in the *ex vivo*-engineered tissue.

It is obvious that the addition of smooth muscle cells would also be of interest, to better reproduce an esophageal wall-like conduit. However, it also introduced technical difficulties to overcome, since conditions for clinical grade expansion of smooth muscle cells are less well defined than for skeletal myoblasts, and the ratio of skeletal myoblasts and smooth muscle cells to be used in the tissue are not yet defined. Moreover, in view of an autologous use, smooth muscle cells should be isolated from an intestinal biopsy with a high risk of whole organ perforation. However, although technical problems are not resolved, it deserves future works to determine their interest in this model.

Our ultimate goal is to be able to apply this procedure to esophageal replacement in human. This requires acceptable and accessible autologous cell sources as well as strict codified procedures (clinically upgraded). As stated above, the gap of organ replacement in humans has already been bridged for tracheal, bladder, and skin replacement.[13–15] The hybrid approach, required for complex tissue creation, is not yet applied for intestinal replacement. Ability to maintain a tubularized form, to avoid structure and to develop a peristaltic capacity, is obviously not possible without cellular components. Even though the aim of our study was to prepare an esophageal substitute, it is important to note that myoblasts have no organ specificity and future substitute can be rendered transferrable to other whole organ replacement taking into account the specificity and nature of the epithelial component (intestinal, urinary conduct, or bile duct). To obtain a complex tissue whose histomorphological qualities are nearest as possible to native tissue, including cell three-dimensional distribution in the scaffold and their coherent behavior and functionality, adequate and appropriate environments and culture conditions are required.

In this model, we demonstrated the feasibility of culturing porcine and HSMs and porcine OECs on acellular scaffolds. The optimal cell culture duration on scaffolds before *in vivo* implantation was 7 days, whatever the cell type. Longer myoblast culture duration did not bring any advantage in terms of cell number and induced cell differentiation and cell fusion, which theoretically have to be avoided. Myoblast of both sources should be seeded at 0.5×10^6 cells/cm^2. For porcine OECs, an initial concentration of 10^6 cells/cm^2 is preferable to obtain a consequent amount of cells on the HAM at D7. The total duration for *in vitro* substitute preparation is 21 days (14 days for cell expansion and 7 days for scaffold culture), compatible with a program of autologous transplantation in animal models and in humans.

Acknowledgments

Funding for this work was provided by the Fondation de l'Avenir grant ETO-579, the Association Française de l'Atrésie de l'Oesophage (AFAO), and Thermo Fisher Scientific.

Tigran Poghosyan and Sebastien Gaujoux were supported by a training grant from the Association Benoît Malassagne.

Disclosure Statement

The authors declare that no competing financial interests exist.

References

1. Bothereau, H., Munoz-Bongrand, N., Lambert, B., Montemagno, S., Cattan, P., and Sarfati, E. Esophageal reconstruction after caustic injury: is there still a place for right coloplasty? Am J Surg **193,** 660, 2007.
2. Chirica, M., de Chaisemartin, C., Munoz-Bongrand, N., Halimi, B., Celerier, M., Cattan, P., and Sarfati, E. [Colonic interposition for esophageal replacement after caustic ingestion]. J Chir (Paris) **146,** 240, 2009.
3. Chirica, M., Veyrie, N., Munoz-Bongrand, N., Zohar, S., Halimi, B., Celerier, M., Cattan, P., and Sarfati, E. Late morbidity after colon interposition for corrosive esophageal injury: risk factors, management, and outcome. A 20-years experience. Ann Surg **252,** 271, 2010.
4. Hulscher, J.B., van Sandick, J.W., de Boer, A.G., Wijnhoven, B.P., Tijssen, J.G., Fockens, P., Stalmeier, P.F., ten Kate, F.J., van Dekken, H., Obertop, H., Tilanus, H.W., and van Lanschot, J.J. Extended transthoracic resection compared with limited transhiatal resection for adenocarcinoma of the esophagus. N Engl J Med **347,** 1662, 2002.
5. Seguier-Lipszyc, E., Bonnard, A., Aizenfisz, S., Enezian, G., Maintenant, J., Aigrain, Y., and de Lagausie, P. The management of long gap esophageal atresia. J Pediatr Surg **40,** 1542, 2005.
6. Poghosyan, T., Gaujoux, S., Chirica, M., Munoz-Bongrand, N., Sarfati, E., and Cattan, P. Functional disorders and quality of life after esophagectomy and gastric tube reconstruction for cancer. J Visc Surg **148,** e327, 2011.
7. Gossot, D., and Lefebvre, J.F. Ischaemic atrophy of the cervical portion of a substernal colic transplant: successful reconstruction using a synthetic resorbable tube. Br J Surg **75,** 801, 1988.
8. Freud, E., Efrati, I., Kidron, D., Finally, R., and Mares, A.J. Comparative experimental study of esophageal wall regeneration after prosthetic replacement. J Biomed Mater Res **45,** 84, 1999.
9. Macchiarini, P., Mazmanian, G.M., de Montpreville, V., Dulmet, E., Fattal, M., Lenot, B., Chapelier, A., and Dartevelle, P. Experimental tracheal and tracheoesophageal allotransplantation. Paris-Sud University Lung Transplantation Group. J Thorac Cardiovasc Surg **110,** 1037, 1995.
10. Gaujoux, S., Le Balleur, Y., Bruneval, P., Larghero, J., Lecourt, S., Domet, T., Lambert, B., Zohar, S., Prat, F., and Cattan, P. Esophageal replacement by allogenic aorta in a porcine model. Surgery **148,** 39, 2010.

11. Horvath, O.P., Cseke, L., Borbely, L., Vereczkei, A., Hobor, B., and Lukacs, L. Skin tube esophagus: present indications and late malignization. Dis Esophagus **13,** 251, 2000.
12. Poghosyan, T., Gaujoux, S., Sfeir, R., Larghero, J., and Cattan, P. Bioartificial oesophagus in the era of tissue engineering. J Pediatr Gastroenterol Nutr **52 Suppl 1,** S16, 2011.
13. Atala, A., Bauer, S.B., Soker, S., Yoo, J.J., and Retik, A.B. Tissue-engineered autologous bladders for patients needing cystoplasty. Lancet **367,** 1241, 2006.
14. Macchiarini, P., Jungebluth, P., Go, T., Asnaghi, M.A., Rees, L.E., Cogan, T.A., Dodson, A., Martorell, J., Bellini, S., Parnigotto, P.P., Dickinson, S.C., Hollander, A.P., Mantero, S., Conconi, M.T., and Birchall, M.A. Clinical transplantation of a tissue-engineered airway. Lancet **372,** 2023, 2008.
15. Kirsner, R.S., Marston, W.A., Snyder, R.J., Lee, T.D., Cargill, D.I., and Slade, H.B. Spray-applied cell therapy with human allogeneic fibroblasts and keratinocytes for the treatment of chronic venous leg ulcers: a phase 2, multicentre, double-blind, randomised, placebo-controlled trial. Lancet**380,** 977, 2012.
16. Saxena, A.K., Kofler, K., Ainodhofer, H., and Hollwarth, M.E. Esophagus tissue engineering: hybrid approach with esophageal epithelium and unidirectional smooth muscle tissue component generation *in vitro*. J Gastrointest Surg **13,** 1037, 2009.
17. Nakase, Y., Nakamura, T., Kin, S., Nakashima, S., Yoshikawa, T., Kuriu, Y., Sakakura, C., Yamagishi, H., Hamuro, J., Ikada, Y., Otsuji, E., and Hagiwara, A. Intrathoracic esophageal replacement by *in situ* tissue-engineered esophagus. J Thorac Cardiovasc Surg **136,** 850, 2008.
18. Badylak, S.F. Xenogeneic extracellular matrix as a scaffold for tissue reconstruction. Transpl Immunol **12,** 367, 2004.
19. Badylak, S.F., Weiss, D.J., Caplan, A., and Macchiarini, P. Engineered whole organs and complex tissues. Lancet **379,** 943, 2012.
20. Mase, V.J., Jr., Hsu, J.R., Wolf, S.E., Wenke, J.C., Baer, D.G., Owens, J., Badylak, S.F., and Walters, T.J. Clinical application of an acellular biologic scaffold for surgical repair of a large, traumatic quadriceps femoris muscle defect. Orthopedics **33,** 511, 2010.
21. Kesting, M.R., Wolff, K.D., Nobis, C.P., and Rohleder, N.H. Amniotic membrane in oral and maxillofacial surgery. Oral Maxillofac Surg, 2012. [Epub ahead of print]; DOI: 10.1007/s10006-012-0382-1.
22. Vilquin, J.T., Marolleau, J.P., Sacconi, S., Garcin, I., Lacassagne, M.N., Robert, I., Ternaux, B., Bouazza, B., Larghero, J., and Desnuelle, C. Normal growth and regenerating ability of myoblasts from unaffected muscles of facioscapulohumeral muscular dystrophy patients. Gene Ther **12,** 1651, 2005.
23. Beckstead, B.L., Pan, S., Bhrany, A.D., Bratt-Leal, A.M., Ratner, B.D., and Giachelli, C.M. Esophageal epithelial cell interaction with synthetic and natural scaffolds for tissue engineering. Biomaterials **26,** 6217, 2005.
24. Hopkinson, A., Shanmuganathan, V.A., Gray, T., Yeung, A.M., Lowe, J., James, D.K., and Dua, H.S. Optimization of amniotic membrane (AM) denuding for tissue engineering. Tissue Eng Part C Methods **14,** 371, 2008.
25. Lopes, M.F., Cabrita, A., Ilharco, J., Pessa, P., Paiva-Carvalho, J., Pires, A., and Patricio, J. Esophageal replacement in rat using porcine intestinal submucosa as a patch or a tube-shaped graft. Dis Esophagus **19,** 254, 2006.
26. Doede, T., Bondartschuk, M., Joerck, C., Schulze, E., and Goernig, M. Unsuccessful alloplastic esophageal replacement with porcine small intestinal submucosa. Artif Organs **33,** 328, 2009.
27. Badylak, S., Meurling, S., Chen, M., Spievack, A., and Simmons-Byrd, A. Resorbable bioscaffold for esophageal repair in a dog model. J Pediatr Surg **35,** 1097, 2000.
28. Marzaro, M., Vigolo, S., Oselladore, B., Conconi, M.T., Ribatti, D., Giuliani, S., Nico, B., Perrino, G., Nussdorfer, G.G., and Parnigotto, P.P. *In vitro* and *in vivo* proposal of an artificial esophagus. J Biomed Mater Res A **77,** 795, 2006.
29. Badylak, S.F., Vorp, D.A., Spievack, A.R., Simmons-Byrd, A., Hanke, J., Freytes, D.O., Thapa, A., Gilbert, T.W., and Nieponice, A. Esophageal reconstruction with ECM and muscle tissue in a dog model. J Surg Res **128,** 87, 2005.
30. Zhu, Y., and Chan-Park, M.B. Density quantification of collagen grafted on biodegradable polyester: its application to esophageal smooth muscle cell. Anal Biochem **363,** 119, 2007.
31. Beauchamp, J.R., Heslop, L., Yu, D.S., Tajbakhsh, S., Kelly, R.G., Wernig, A., Buckingham, M.E., Partridge, T.A., and Zammit, P.S. Expression of CD34 and Myf5 defines the majority of quiescent adult skeletal muscle satellite cells. J Cell Biol **151,** 1221, 2000.
32. Relaix, F., and Marcelle, C. Muscle stem cells. Curr Opin Cell Biol **21,** 748, 2009.
33. Partridge, T.A., Morgan, J.E., Coulton, G.R., Hoffman, E.P., and Kunkel, L.M. Conversion of mdx myofibres from dystrophin-negative to -positive by injection of normal myoblasts. Nature **337,** 176, 1989.
34. Arcila, M.E., Ameredes, B.T., DeRosimo, J.F., Washabaugh, C.H., Yang, J., Johnson, P.C., and Ontell, M. Mass and functional capacity of regenerating muscle is enhanced by myoblast transfer. J Neurobiol **33,** 185, 1997.
35. Menasche, P., Hagege, A.A., Scorsin, M., Pouzet, B., Desnos, M., Duboc, D., Schwartz, K., Vilquin, J.T., and Marolleau, J.P. Myoblast transplantation for heart failure. Lancet **357,** 279, 2001.
36. Menasche, P., Alfieri, O., Janssens, S., McKenna, W., Reichenspurner, H., Trinquart, L., Vilquin, J.T., Marolleau, J.P., Seymour, B., Larghero, J., Lake, S., Chatellier, G., Solomon, S., Desnos, M., and Hagege, A.A. The Myoblast Autologous Grafting in Ischemic Cardiomyopathy (MAGIC) trial: first randomized placebo-controlled study of myoblast transplantation. Circulation **117,** 1189, 2008.
37. Ohki, T., Yamato, M., Murakami, D., Takagi, R., Yang, J., Namiki, H., Okano, T., and Takasaki, K. Treatment of oesophageal ulcerations using endoscopic transplantation of tissue-engineered autologous oral mucosal epithelial cell sheets in a canine model. Gut **55,** 1704, 2006.
38. Wei, R.Q., Tan, B., Tan, M.Y., Luo, J.C., Deng, L., Chen, X.H., Li, X.Q., Zuo, X., Zhi, W., Yang, P., Xie, H.Q., and Yang, Z.M. Grafts of porcine small intestinal submucosa with cultured autologous oral mucosal epithelial cells for esophageal repair in a canine model. Exp Biol Med (Maywood) **234,** 453, 2009.
39. Hayashi, K., Ando, N., Ozawa, S., Kitagawa, Y., Miki, H., Sato, M., and Kitajima, M. A neo-esophagus reconstructed by cultured human esophageal epithelial cells, smooth muscle cells, fibroblasts, and collagen. ASAIO J **50,** 261, 2004.
40. Kofler, K., Ainoedhofer, H., Hollwarth, M.E., and Saxena, A.K. Fluorescence-activated cell sorting of PCK-26 antigen-positive cells enables selection of ovine esophageal epithelial cells with improved viability on scaffolds for esophagus tissue engineering. Pediatr Surg Int **26,** 97, 2010.

41. Wolf, M.T., Daly, K.A., Reing, J.E., and Badylak, S.F. Biologic scaffold composed of skeletal muscle extracellular matrix. Biomaterials **33,** 2916, 2012.
42. Hirai, H., Verma, M., Watanabe, S., Tastad, C., Asakura, Y., and Asakura, A. MyoD regulates apoptosis of myoblasts through microRNA-mediated down-regulation of Pax3. J Cell Biol **191,** 347, 2010.
43. Tajbakhsh, S., Rocancourt, D., Cossu, G., and Buckingham, M. Redefining the genetic hierarchies controlling skeletal myogenesis: Pax-3 and Myf-5 act upstream of MyoD. Cell **89,** 127, 1997.
44. Olguin, H.C., and Pisconti, A. Marking the tempo for myogenesis: Pax7 and the regulation of muscle stem cell fate decisions. J Cell Mol Med **16,** 1013, 2012.
45. Olguin, H.C., and Olwin, B.B. Pax-7 up-regulation inhibits myogenesis and cell cycle progression in satellite cells: a potential mechanism for self-renewal. Dev Biol **275,** 375, 2004.
46. Zammit, P.S., Relaix, F., Nagata, Y., Ruiz, A.P., Collins, C.A., Partridge, T.A., and Beauchamp, J.R. Pax7 and myogenic progression in skeletal muscle satellite cells. J Cell Sci **119,** 1824, 2006.
47. Green, N., Huang, Q., Khan, L., Battaglia, G., Corfe, B., MacNeil, S., and Bury, J.P. The development and characterization of an organotypic tissue-engineered human esophageal mucosal model. Tissue Eng Part A **16,** 1053, 2010.
48. Meller, D., and Tseng, S.C. [Reconstruction of the conjunctival and corneal surface. Transplantation of amnionic membrane]. Ophthalmologe **95,** 805, 1998.

Address correspondence to:
Pierre Cattan, MD, PhD
Department of Digestive and Endocrine Surgery
Saint-Louis Hospital, APHP
University Paris 7
1, avenue Claude-Vellefaux -75475 PARIS Cedex 10
France

E-mail: pierre.cattan@sls.aphp.fr

Received: September17, 2012
Accepted: April25, 2013
Online Publication Date: June 25, 2013